



ELSEVIER

Contents lists available at ScienceDirect

Optics Communications

journal homepage: [www.elsevier.com/locate/optcom](http://www.elsevier.com/locate/optcom)

Invited Paper

# Optically tunable full 360° microwave photonic phase shifter using three cascaded silicon-on-insulator microring resonators



Nasrin Ehteshami, Weifeng Zhang, Jianping Yao\*

Microwave Photonics Research Laboratory, School of Electrical Engineering and Computer Science, University of Ottawa, Ottawa, ON, Canada, K1N 6N5

## ARTICLE INFO

## Article history:

Received 16 March 2015

Received in revised form

18 August 2015

Accepted 21 August 2015

Available online 11 September 2015

## Keywords:

Silicon ring resonator

Phase shifter

Microwave photonics

Thermal nonlinear effect

## ABSTRACT

A broadband optically tunable microwave phase shifter with a tunable phase shift covering the entire 360° range using three cascaded silicon-on-insulator (SOI) microring resonators (MRRs) that are optically pumped is proposed and experimentally demonstrated. The phase tuning is implemented based on the thermal nonlinear effect in the MRRs. By optically pumping the MRRs, the stored light in the MRRs is absorbed due to two photon absorption (TPA) to generate free carriers, which result in free carrier absorption (FCA). The FCA effect would lead to the heating of the MRRs and cause a redshift in the phase response, which is used to implement a microwave phase shifter with a tunable phase shift. The device is designated and fabricated on an SOI platform, which is experimentally evaluated. The experimental results show that by optically pumping the MRRs, a broadband microwave photonic phase shifter with a bandwidth of 7 GHz from 16 to 23 GHz with a tunable phase shift covering the entire 360° phase shift range is achieved.

Crown Copyright © 2016 Published by Elsevier B.V. All rights reserved.

## 1. Introduction

Broadband microwave phase shifters are one of the key components in microwave systems for applications such as in phased array antennas, arrayed signal processors, and microwave filters [1,2]. Thanks to the ultra-wideband offered by photonics [3], a microwave phase shifter implemented based on photonics can operate at a higher frequency with a bandwidth that is wider than that of a pure electronic microwave phase shifter [4]. For instance, a microwave photonic phase shifter with a phase shift of 114° at 3 GHz was obtained by using a distributed-feedback (DFB) laser through optical wavelength conversion [5]. By cascading two semiconductor optical amplifiers (SOAs), a microwave photonic phase shifter with a phase shift of 240° at a microwave frequency of 19 GHz based on the slow- and fast-light effects was demonstrated [6]. For an SOA-based microwave photonic phase shifter, to achieve a large phase shift, multiple SOAs should be used, which may make the system complicated. A simple approach to implementing a microwave photonic phase shifter is to use a tilted fiber Bragg grating (TFBG) co-doped with erbium and ytterbium (Er/Yb) [7]. A tunable phase shift from +140° to −140° was achieved by pumping the TFBG with a 980-nm laser diode (LD) with a tuning pumping power from 30 to 95 mW. The bandwidth was as wide as 12 GHz, from 24 to 36 GHz. The phase shifters

reported in [5–7], however, were implemented using discrete components with very large size and poor stability. To reduce the size and improve the stability, integration would be highly needed [8]. Recently, microwave phase shifters implemented based on integrated silicon chips were reported [9–12]. An electrically tunable microwave photonic phase shifter using a single silicon-on-insulator microring resonator (SOI-MRR) or two cascaded SOI-MRRs with a phase shift of 204° or 360° at 40 GHz was demonstrated [9,10]. The phase tuning was implemented using an embedded micro-heater. Since the phase shift was achieved at a single frequency, the phase shifter in [9,10] was, in fact, a true time delay line. In [11], a true phase shifter based on separate carrier tuning using two cascaded SOI-MRRs was demonstrated. Again, the tuning was done using a micro-heater. In [12], an all-optically tunable microwave photonic phase shifter with a phase shift of 260° was achieved by using a single passive MRR. The tuning was realized by utilizing the thermal nonlinear effect due to two photon absorption (TPA) in the silicon MRR. The advantage is that no micro-heater is needed, which simplifies the design and fabrication. However, due to the limited phase tuning range, it is difficult to realize a full 360° phase shift using a single MRR. For many applications, a full 360° phase shift is needed. For example, when implementing microwave photonic filters [13,14], microwave phase shifters with a full 360° phase shift is needed.

In this paper, we propose and experimentally demonstrate a full 360° optically tunable phase shifter based on three cascaded passive MRRs. A microwave signal to be phase shifted is applied to an optical single-sideband (OSSB) modulator to generate an optical

\* Corresponding author.

E-mail address: [jpyao@eecs.uottawa.ca](mailto:jpyao@eecs.uottawa.ca) (J. Yao).

carrier and an optical sideband. The phase shift is introduced to the optical carrier by placing the optical carrier within the bandwidth of one resonance of the cascaded MRRs. The phase tuning is implemented based on the thermal nonlinear effect in the MRRs. By optically pumping the MRRs, the stored light in the MRRs is absorbed due to two photon absorption (TPA), to generate free carriers, which result in free carrier absorption (FCA). The effect leads to the heating of the MRRs, which cause a redshift in the phase response and are used to introduce a tunable phase shift. The device is designated and fabricated on an SOI platform, which is experimentally evaluated. The experimental results show that by pumping the MRRs, a broadband microwave phase shifter with a bandwidth of 7 GHz from 16 to 23 GHz with a phase shift covering the entire  $360^\circ$  range is achieved.

## 2. Principle of operation

Fig. 1 shows the schematic of a microwave photonic phase shifter using an SOI MRR. A microwave signal to be phase shifted is modulated on an optical carrier at an OSSB modulator. The OSSB-modulated signal is then sent to an SOI-MRR with the optical carrier located within the bandwidth of one of the MRR resonances to introduce a phase shift to the optical carrier. After photodetection at a photodetector (PD), the phase shift is translated to the microwave signal.

Mathematically, under small-signal modulation condition, the optical field at the output of the OSSB modulator (point B) can be expressed as

$$E_{in}(t) = A_0 \exp(j\omega_0 t) + A_1 \exp[j(\omega_0 + \omega_{rf})t] \quad (1)$$

where  $A_0$  and  $\omega_0$  are the amplitude and the frequency of the optical carrier, respectively, and  $A_1$  and  $\omega_0 + \omega_{rf}$  are the amplitude and frequency of the first-order sideband, respectively. The optical field at the output of the SOI MRR (point C) is given by [10]

$$E_{out}(t) = A_0 B \exp(j\omega_0 t) \exp(j\theta_0) + A_1 B' \exp[j(\omega_0 + \omega_{rf})t] \quad (2)$$

where  $B$  and  $B'$  are, respectively, the amplitudes of the MRR spectral response at  $\omega_0$  and  $\omega_0 + \omega_{rf}$ , and  $\theta_0$  is the phase shift at  $\omega_0$  of the MRR spectral response. The phase shifted optical carrier and the first-order sideband are then applied to the PD. The beating between these two components will generate a microwave signal (point D) with a phase shift equal to the phase difference between the optical carrier and the first-order sideband. The phase-shifted microwave signal is given by

$$i_{RF}(t) = R |E_{out}(t)|^2 = RA_0 A_1 B B' \cos(\omega_{rf} t + \theta_0) \quad (3)$$

where  $R$  is the responsivity of the PD. As can be seen from (3), the

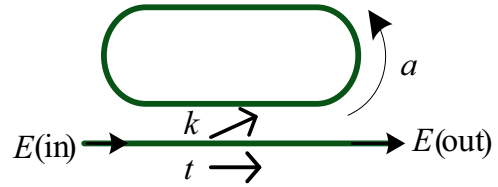


Fig. 2. The schematic of an all-pass single MRR.

phase shift introduced to the optical carrier by the SOI MRR is directly translated to the microwave signal. The value of the phase shift is optically tunable by optically pumping the SOI MRR which would cause a continuous lateral shift of the spectral response and consequently a phase shift. The key component in the microwave phase shifter is the cascaded MRRs which are fabricated on an SOI platform.

First, we study the operation of a single MRR and its application to introduce a phase shift. Fig. 2 shows the schematic of an all-pass single MRR, where  $k$  and  $a$  are the amplitude coupling coefficient and the roundtrip amplitude transmission coefficient, respectively. The transfer function at the through port can be expressed as [15],

$$\frac{E_{out}}{E_{in}} = \left[ \frac{t - a \exp(j\varphi)}{1 - ta \exp(j\varphi)} \right] \quad (4)$$

where  $t$  is the amplitude transmission coefficient of the coupling region which satisfies the relation  $t^2 + k^2 = 1$  for lossless coupling,  $a = \exp(-\alpha L/2)$ , where  $L$  and  $\alpha$  are the length and the linear loss of the ring, respectively.  $\varphi = \beta L$  is the round-trip phase change of the ring and  $\beta$  is the propagation constant given by  $\beta = kn_{eff} = \frac{2\pi}{\lambda} n_{eff}$ , where  $n_{eff}$  is the effective refractive index of the waveguide and  $\lambda$  is the wavelength. The total phase shift of the transmitted light for one ring is given by

$$\phi = \pi + \varphi + \arctan\left(\frac{t \sin \varphi}{a - t \cos \varphi}\right) + \arctan\left(\frac{at \sin \varphi}{1 - at \cos \varphi}\right) \quad (5)$$

Fig. 3 shows the transmission and the phase response for an MRR at the through port with different coupling coefficients  $k$ . Under the under-coupling and critical-coupling conditions, the phase shift cannot reach the maximum value. To achieve a maximum phase shift the MRR should be designed to operate under the over-coupling condition.

By increasing the number of the cascaded MRRs the phase shift would increase [16]. Fig. 4 shows the simulation result for three cascaded MRRs that are designed to operate in the over-coupling condition. As can be seen the phase shift range is tripled as compared with the use of a single MRR.

The optical tunability of the phase shift  $\theta_0$  in (3) is achieved based on the thermal nonlinear effect where the TPA will happen

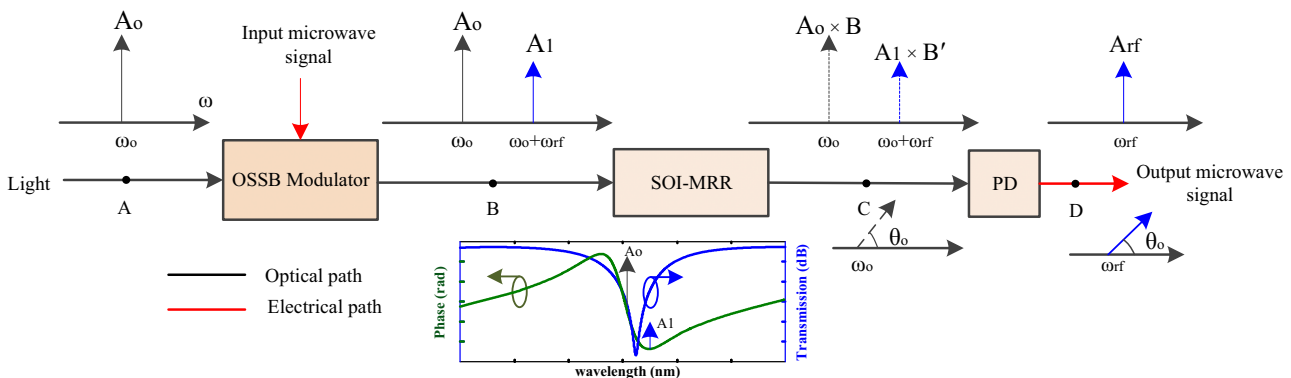
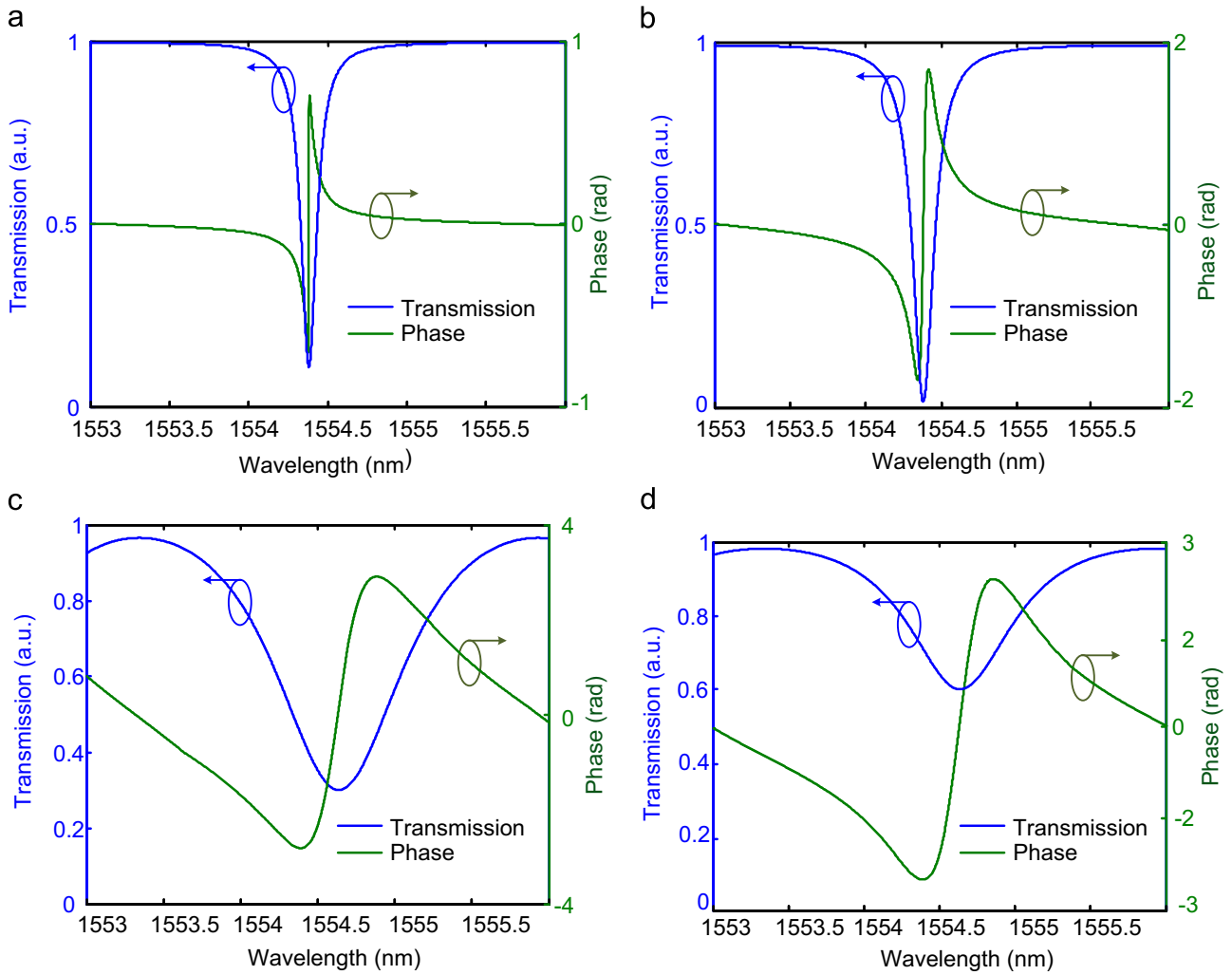
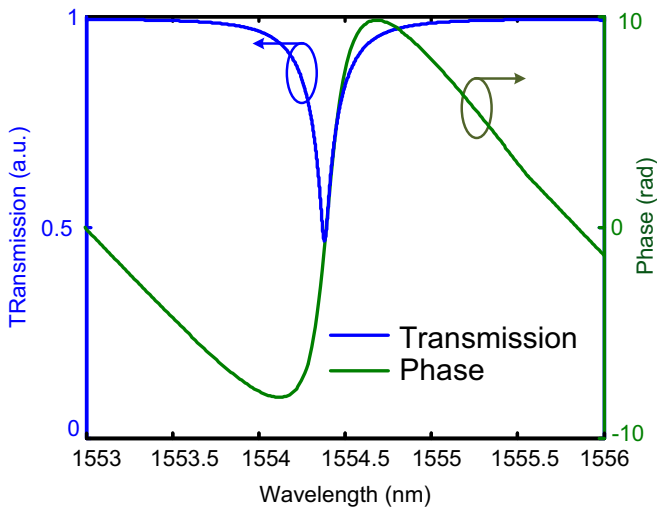


Fig. 1. Schematic of a microwave photonic phase shifter using an SOI MRR. OSSB: optical single-sideband, SOI-MRR: silicon-on-insulator microring resonator, PD: photodetector. Inset: the amplitude and phase responses of the SOI-MRR.



**Fig. 3.** Transmission and phase response at the through port for an MRR under different coupling conditions: (a) under-coupling with  $k=0.06$ , (b) critical-coupling with  $k^2=1-a^2=0.01$ , (c) over coupling with  $k=0.3$ , and (d) over-coupling with  $k=0.4$  ( $a\sim 0.997$ ).



**Fig. 4.** Transmission and phase response at the through port for three cascaded MRRs under the over-coupling condition with  $k=0.4$  ( $a\sim 0.997$ ).

in an MRR if it is pumped optically by a pumping source with its wavelength located at a resonant wavelength of the MRR. The thermal-optic (TO) effect due to the TPA-induced FCA will cause heating of the MRR, and lead to a continuous shift of the spectral

response and consequently  $\theta_0$  can be tunable [17,18]. An optical tunable phase shifter based on one MRR and three cascaded MRRs are discussed and compared in the next Section.

### 3. Experimental results and discussion

An experiment is performed based on the experimental setup shown in Fig. 5. The key component in the proposed microwave photonic phase shifter is the three cascaded MRRs fabricated on an SOI platform. Each MRR has a radius of  $20\ \mu\text{m}$  with a 220-nm-thick silicon slab on top of a 2- $\mu\text{m}$  silica buffer layer. The cross section of the silicon waveguide has a dimension of  $w=500\ \text{nm}$  and  $h=220\ \text{nm}$ , as shown in Fig. 6(a). The coupling length between a MRR and the waveguide is  $10\ \mu\text{m}$  and the coupling gap is 270 nm. Two grating couplers are incorporated to couple the light into the MRRs from a single-mode fiber and out of the MRRs to another single-mode fiber. Fig. 6(b) and (c) shows the images of an MRR and three cascaded MRRs.

A light wave from a laser diode (LD1) is coupled via a polarization controller (PC1) to a Mach-Zehnder modulator (MZM), to which a microwave signal from a vector network analyzer (VNA) is applied via the RF port. An optical double-sideband (ODSB) signal is obtained at the output of the MZM. To suppress one of the two sidebands, a wave-shaper serving as an optical notch filter to suppress one sideband is connected to the output of the MZM and

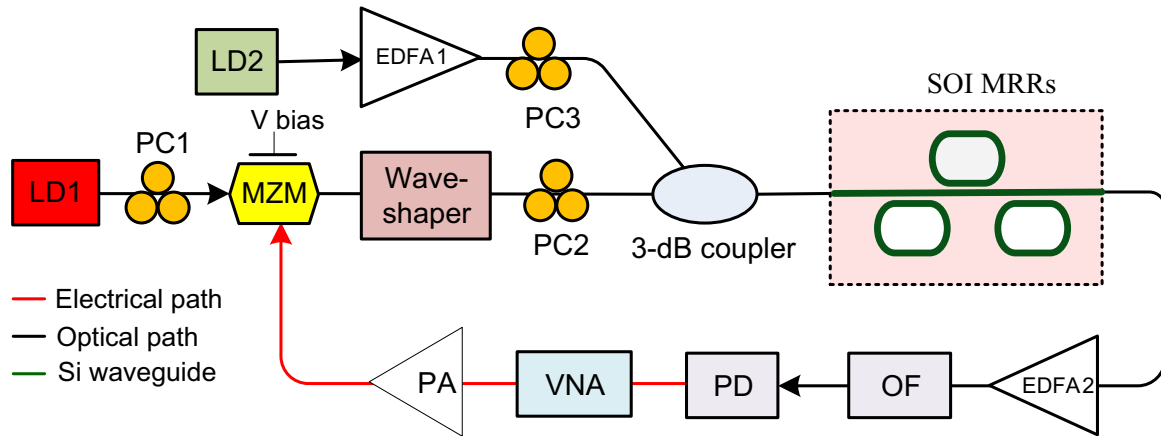


**Fig. 5.** Experimental set up. LD: laser diode, PC: polarization controller, MZM: Mach-Zehnder modulator, EDFA: erbium-doped fiber amplifier, SOI: silicon on insulator, MRR: microring resonator, OF: optical filter, PD: photodetector, VNA: vector network analyzer, PA: power amplifier.

an OSSB-modulated signal is thus obtained. The OSSB-modulated optical signal is then sent to the SOI-MRRs via a second PC (PC2). A pumping light wave from a second LD (LD2) is amplified by an erbium-doped fiber amplifier (EDFA1) and sent to the SOI MRRs via a 3-dB coupler. The MRRs are designed to only support the transverse electric (TE) mode. Thus, during the experiment, PC2 and PC3 are adjusted to ensure that the input signal to the MRRs is TE polarized. The output optical signal of the MRRs is amplified by a second EDFA (EDFA2) and sent to an optical filter (OF) to filter out the residual pumping light before applying to a PD.

Fig. 7(a) shows the measured magnitude and phase responses of an MRR at different pumping power levels of 27, 22, 18 dBm. The response without pumping is also shown. By increasing the pump power, the magnitude and phase responses are shifted to a longer wavelength. By placing the optical carrier of the OSSB signal in the bandwidth of the phase response, a phase shift will be introduced to the optical carrier. As shown in Fig. 7(b), the maximum value of phase difference between the optical carrier and the sideband is  $285^\circ$ . A full  $360^\circ$  phase shift cannot be implemented using a single MRR. To achieve a full  $360^\circ$  phase shift, more than one MRR is needed. Fig. 8 shows the transmission spectrum of the three cascaded MRRs for the TE mode where the spectral range from 1543 to 1549 nm covering two resonance notches at 1544.2 nm and 1548.03 nm. The notch depths for resonance notches are 5 dB and 16 dB, which are not equal due to the wavelength-dependent coupling conditions. The inset gives a zoom-in view of the first

notch at 1543 nm and its phase response. The modulated signal is placed in the bandwidth of the first notch because at this wavelength, the MRRs work in the over-coupling condition, the MRRs will show a maximum phase shift. To demonstrate the tunability of the phase shifter, the wavelength of the pumping light is selected to be at the wavelength of the second resonance notch, 1548.03 nm, to maximize the coupling of the pumping light into the MRRs.

Fig. 9 shows the phase response of the MRRs corresponding to the first notch. The central wavelength of phase response is shifted from about 1544.20 to 1544.26 nm with a total wavelength shift of  $\Delta\lambda=0.06$  nm by changing the pumping power from 0 (no pump) to 27 dBm. A maximum phase shift of  $855^\circ$  is achieved. To realize a full  $360^\circ$  microwave phase shift, the optical carrier is set at  $\lambda=1544.26$  nm. By increasing pump power, the phase difference between the carrier and the sideband is also increasing. When the pump power is 27 dBm, the phase difference between optical carrier and sideband reaches its maximum value. This tunable phase shift can be used to introduce a tunable phase shift to the optical carrier of the OSSB-modulated signal to obtain a phase-shifted microwave signal when the OSSB-modulated signal is detected at the PD. Fig. 10 shows the phase shift measured using a VNA at different microwave frequencies. As can be seen, a full  $360^\circ$  phase shift with a bandwidth of 7 GHz from 16 to 23 GHz is achieved. As expected, the phase shift is independent of the microwave frequency. This confirms that the system is a microwave phase shifter, rather than a true time delay line.

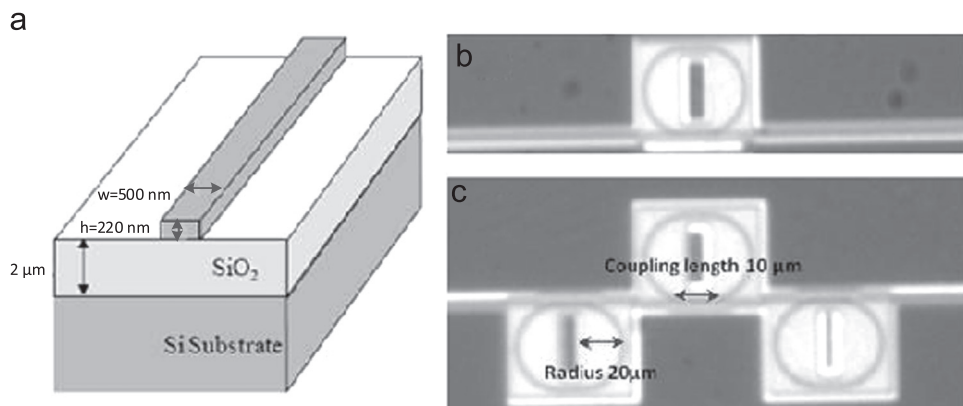


**Fig. 6.** (a) The side view of a silicon waveguide on an SOI wafer. (b) An image of the fabricated single MRR. (c) An image of the fabricated 3 cascaded MRRs.

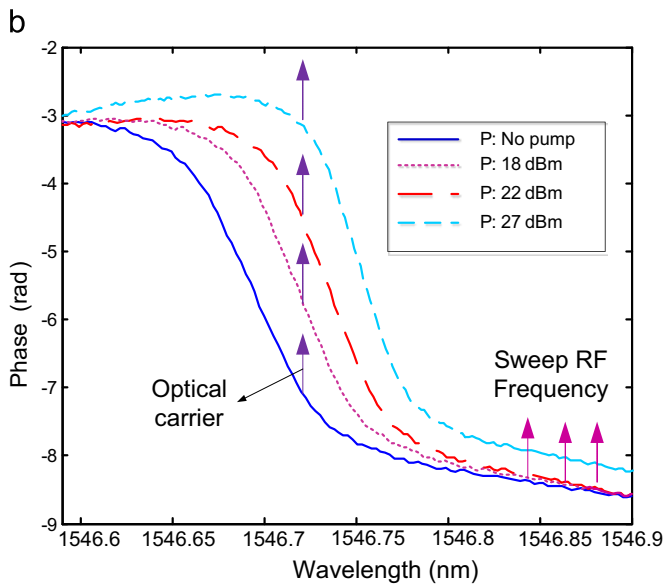
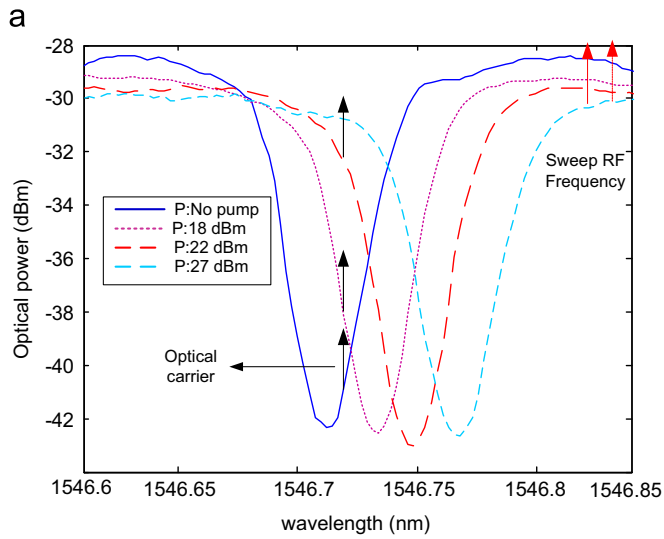


Fig. 7. (a) The magnitude response, and (b) the phase response of a single MRR showing a net redshift of the magnitude and phase with the increase of the pump power from 0 (no pump) to 27 dBm.

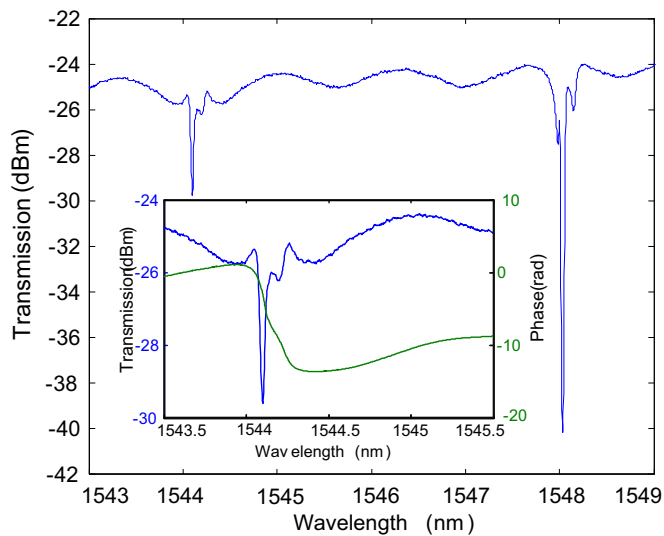


Fig. 8. Transmission spectrum of the three cascaded MRRs for the TE mode. Inset: a zoom-in view of the first notch and corresponding phase response.

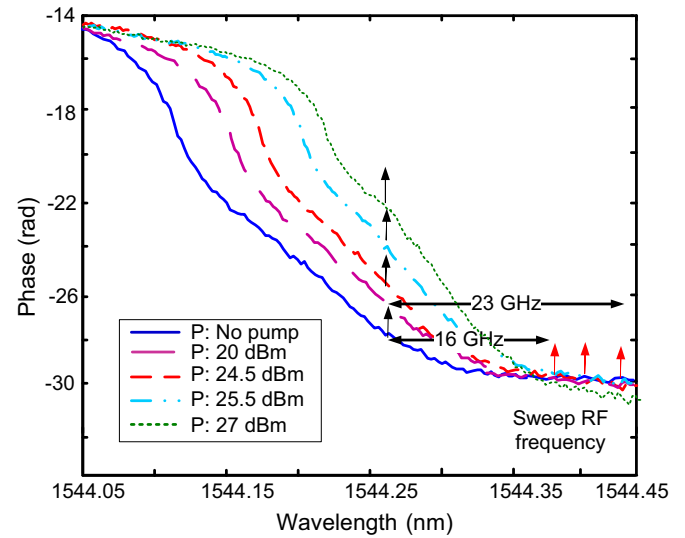


Fig. 9. The phase response of the three cascaded MRRs showing a net redshift of the phase response with the increase of the pumping power from 0 (no pump) to 27 dBm.

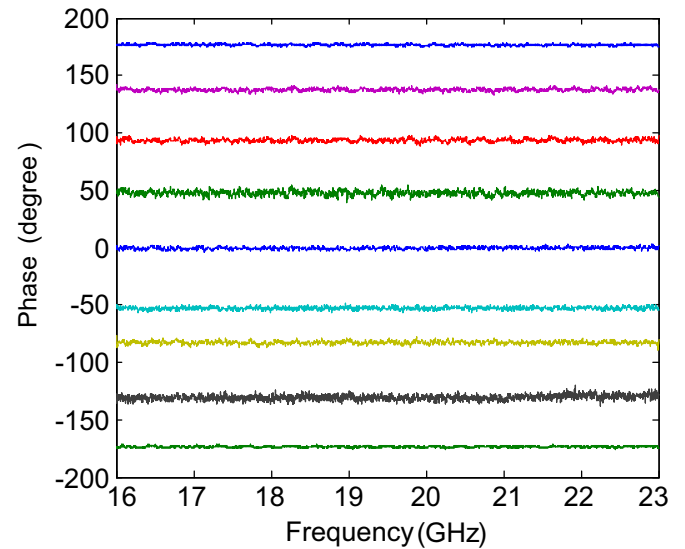


Fig. 10. Measured phase shifts at different pumping power levels. The phase shifts are independent of the microwave frequency.

In the experiment, the phase shifter has a bandwidth of 7 GHz from 16 to 23 GHz. The upper frequency of 23 GHz is limited by the bandwidth of the PD (here the bandwidth of the PD was 25 GHz). For the proposed phase shifter, if a PD with a much wider bandwidth is used, then the highest frequency will only be limited by the wavelength spacing between two adjacent resonance peaks which is about 4 nm or 500 GHz for the fabricated MRRs. The lower frequency of 16 GHz is limited by the notch width of the cascaded MRRs. If the MRRs have a narrower notch, the lower frequency can be smaller.

Note that for a microwave phase shifter, we expect the power of the phase-shifted microwave signal at the output of the phase shifter is constant when the phase shift is tuned. In the proposed approach, the power variation is maintained small by slightly offsetting the resonance wavelengths of the three cascaded MRRs. As can be seen in the inset in Fig. 8, the notch depth is 5 dB, which is smaller than that of a single MRR. When the optical carrier is set at  $\lambda = 1544.26$  nm, the amplitude difference between location of the optical carrier and sideband is less than 1 dB which leads to low range of microwave power fluctuations at the output of the PD.

#### 4. Conclusions

An all-optically tunable microwave photonic phase shifter based on three cascaded SOI MRRs was proposed and experimentally demonstrated. The phase tuning was implemented by tuning the phase response of the MRRs through optical pumping. Due to the TPA-induced TO effect, the phase response was shifted to a longer wavelength, which led to the change of the phase shift of the microwave phase shifter. The SOI MRRs were designed and fabricated on an SOI platform. The use of the fabricated MRRs to implement a broadband microwave photonic phase shifter with a bandwidth of 7 GHz from 16 to 23 GHz with a tunable phase shift covering the entire 360° phase shift range was demonstrated.

#### Acknowledgments

This work was supported by the Natural Sciences and Engineering Research Council of Canada (NSERC). The authors acknowledge CMC Microsystems for providing the design tools and enabling the fabrication through IMEC, ePIXfab.

#### References

- [1] J.P. Yao, *J. Lightwave Technol.* 27 (2009) 314–335.
- [2] J. Capmany, B. Ortega, D. Pastor, S. Sales, *J. Lightwave Technol.* 23 (2005) 702–723.
- [3] R.A. Minasian, E.H.W. Chan, X. Yi, *Opt. Express* 21 (2013) 22918–22936.
- [4] F. De Flaviis, *Encyclopedia of RF and Microwave Engineering*, 2005, (April).
- [5] M. Fisher, S. Chuang, *IEEE Photonics Technol. Lett.* 18 (2006) 1714–1716.
- [6] W. Xue, S. Sales, J. Capmany, J. Mork, *Opt. Lett.* 34 (2009) 929–931.
- [7] H. Shahoei, J.P. Yao, *Opt. Express* 20 (2012) 14009–14014.
- [8] D. Marpaung, C. Roeloffzen, R. Heideman, A. Leinse, S. Sales, J. Capmany, *Laser Photonics Rev.* 7 (2013) 506–538.
- [9] M. Pu, L. Liu, W. Xue, Y. Ding, L.H. Frandsen, H. Ou, K. Yvind, J. Hvam, *IEEE Photonics Technol. Lett.* 22 (2010) 869–871.
- [10] M. Pu, L. Liu, W. Xue, Y. Ding, H. Ou, K. Yvind, J.M. Hvam, *Opt. Express* 18 (2010) 6172–6182.
- [11] M. Burla, D. Marpaung, L. Zhuang, C. Roeloffzen, M.R. Khan, A. Leinse, M. Hoekman, R. Heideman, *Opt. Express* 19 (2011) 21475–21484.
- [12] Q. Chang, Q. Li, Z. Zhang, M. Qiu, T. Ye, Y. Su, *IEEE Photonics Technol. Lett.* 21 (2009) 60–62.
- [13] J. Capmany, B. Ortega, D. Pastor, *J. Lightwave Technol.* 24 (2006) 221–229.
- [14] W. Xue, S. Sales, J. Mork, J. Capmany, *IEEE Photonics Technol. Lett.* 21 (2009) 167–169.
- [15] W. Bogaerts, et al., *Laser Photonics Rev.* 6 (2012) 47–73.
- [16] Y. Chen, S. Blair, *J. Opt. Soc. Am. B.* 20 (2003) 2125–2132.
- [17] Q. Xu, M. Lipson, *Opt. Lett.* 31 (2006) 341–343.
- [18] L.W. Luo, G.S. Wiederhecker, K. Preston, M. Lipson, *Opt. Lett.* 37 (2012) 590–592.